Electronic Supplementary Material (ESI) for Journal of Materials Chemistry A.

Supplementary Information

Monodisperse RuO_2 nanoparticles for highly transparent and rapidly responsive supercapacitor electrodes

Ilhwan Ryu†, Dongju Kim†, Guenpyo Choe, Sohyun Jin, Dajung Hong and Sanggyu Yim**

Department of Chemistry, Kookmin University, Seoul 02707, South Korea

* Corresponding authors: Dajung Hong (solar@kookmin.ac.kr), Sanggyu Yim (sgyim@kookmin.ac.kr)

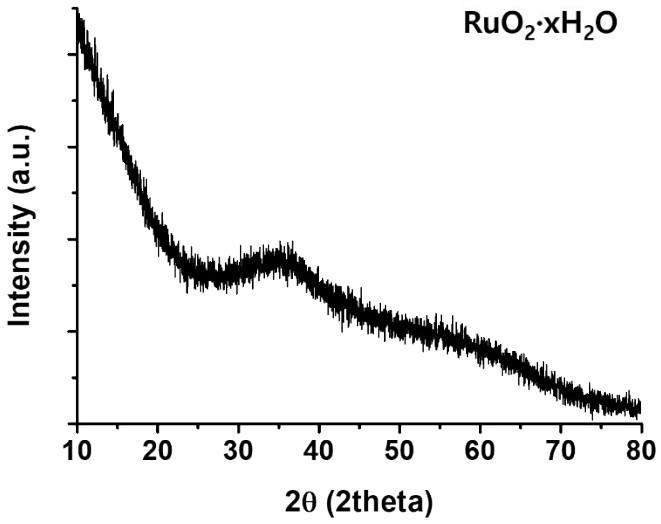

Figure S1. Powder X-ray diffraction pattern of the synthesized pristine RuO_2 NPs.

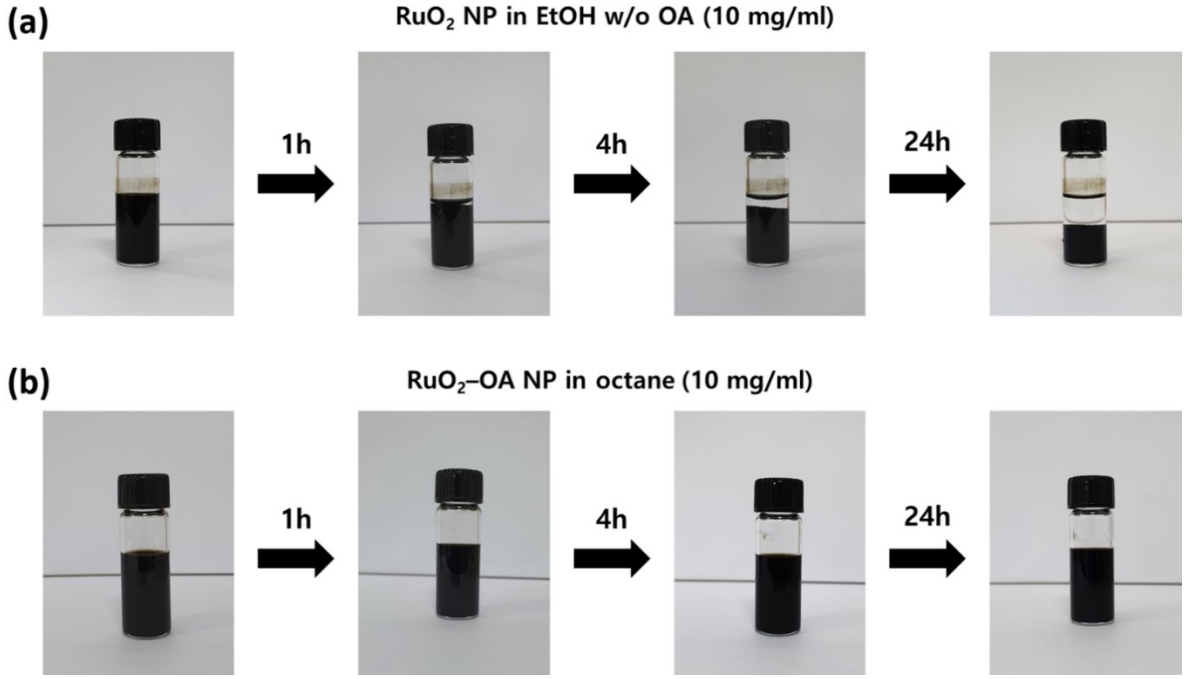

Figure S2. Photographs of (a) pristine RuO_2 NPs dispersed in ethanol and (b) OA-decorated RuO_2 NPs dispersed in octane and taken at various times after dissolution.

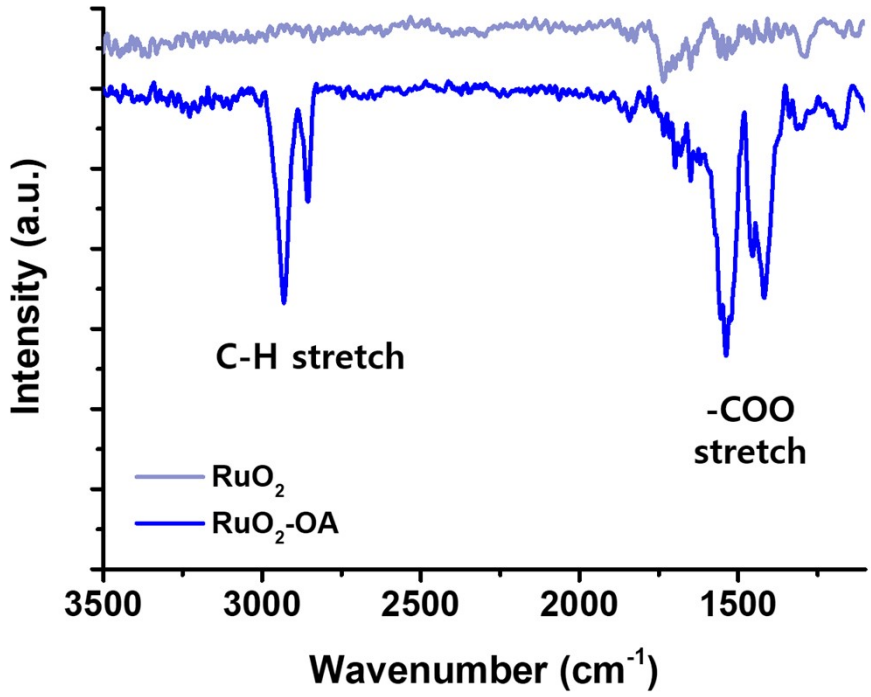

Figure S3. FTIR spectra of the pristine and OA-decorated RuO_2 NP-based electrodes.

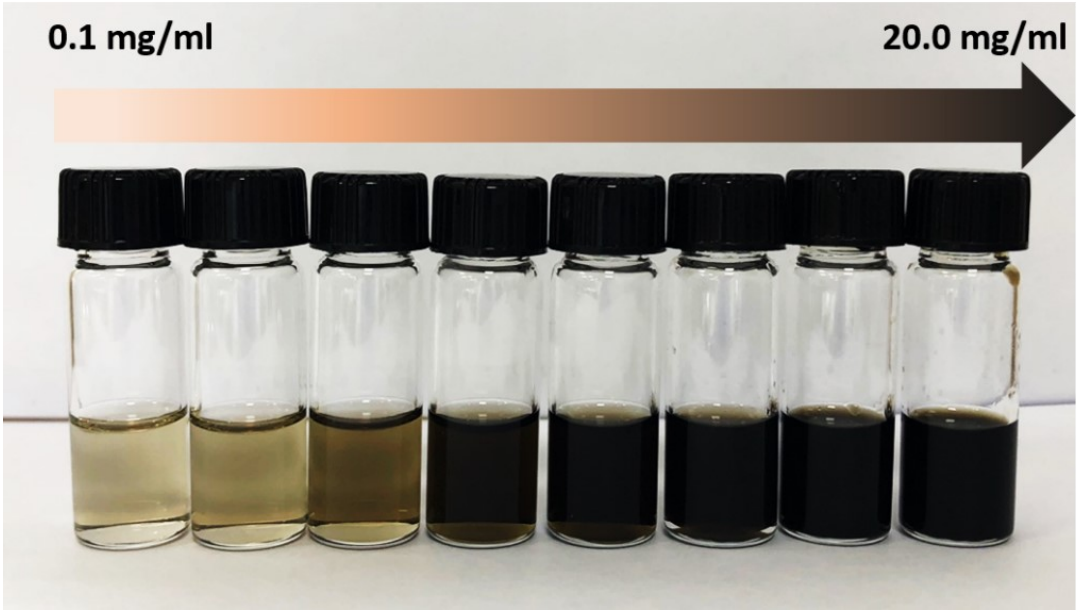

Figure S4. Photograph of OA-decorated RuO_2 NPs of various concentrations (from left to right: 0.1, 0.2, 0.5, 1.0, 2.0, 5.0, 10.0, and 20.0 mg/ml) dispersed in octane. Taken after 24 h of dissolution.

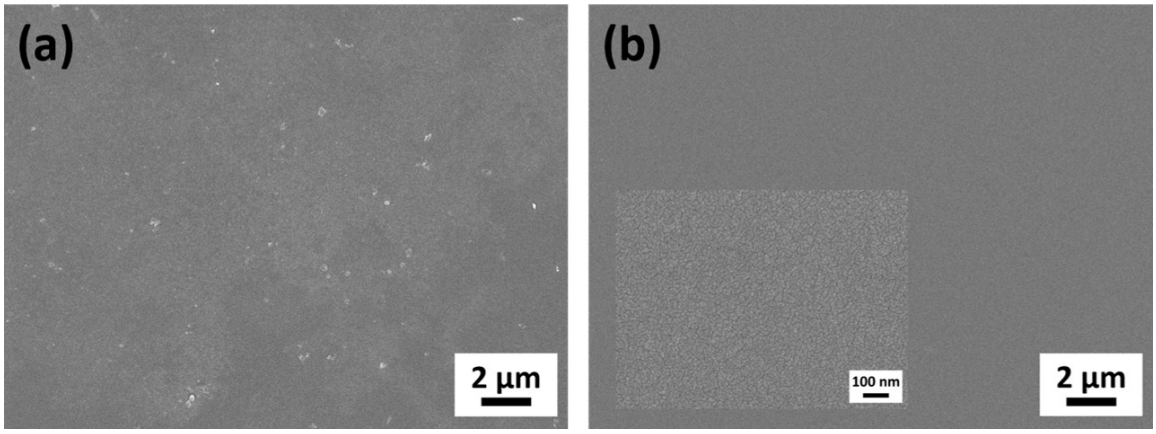

Figure S5. Surface FE-SEM images of thin films spin-coated with 10 mg/ml solution of (a) pristine RuO_2 NPs dispersed in ethanol and (b) OA-decorated RuO_2 NPs dispersed in octane.

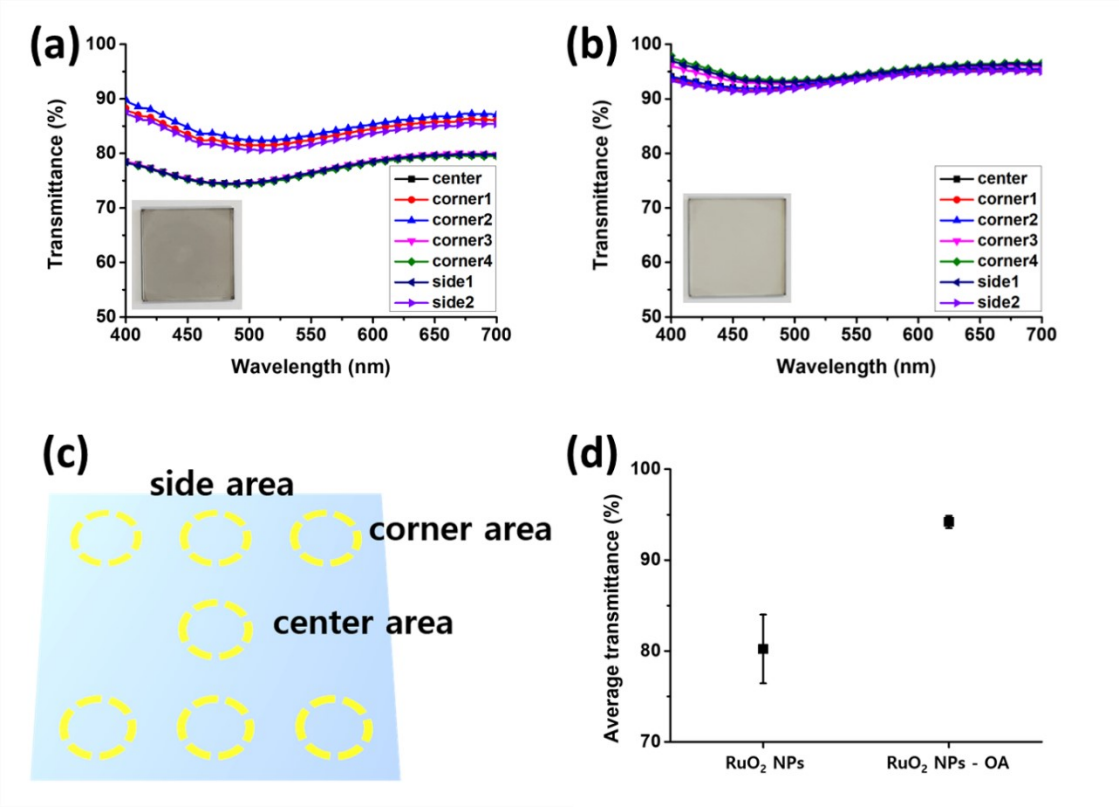

Figure S6. Transmittance spectra of thin films spin-coated with 10 mg/ml solution of (a) pristine RuO_2 NPs dispersed in ethanol and (b) OA-decorated RuO_2 NPs dispersed in octane. (c) Schematic illustrating measurement points on the films. (d) Mean and spread of the average transmittance over the visible wavelength range for pristine RuO_2 and RuO_2–OA NP-coated films.

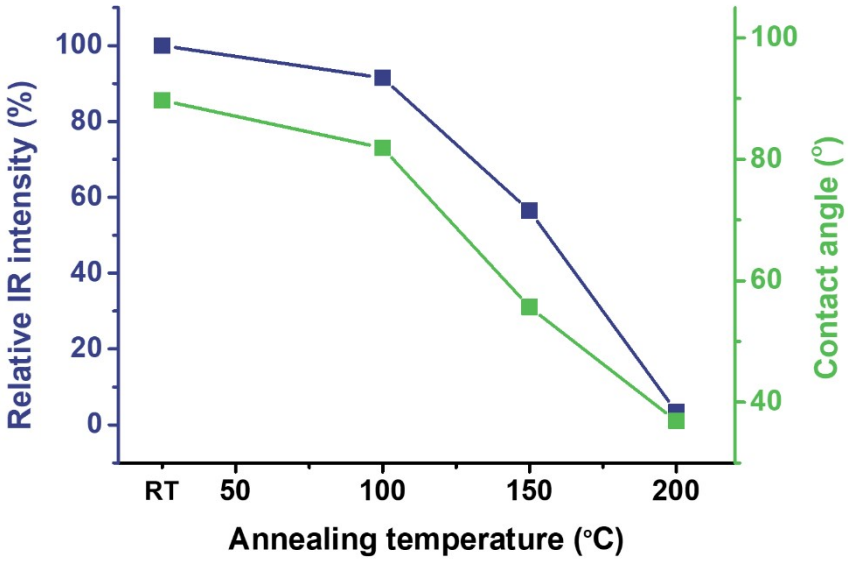

Figure S7. Plots of C–H stretching band intensity in FT-IR and water contact angle of the RuO_2–OA NP-coated films as a function of the annealing temperature.

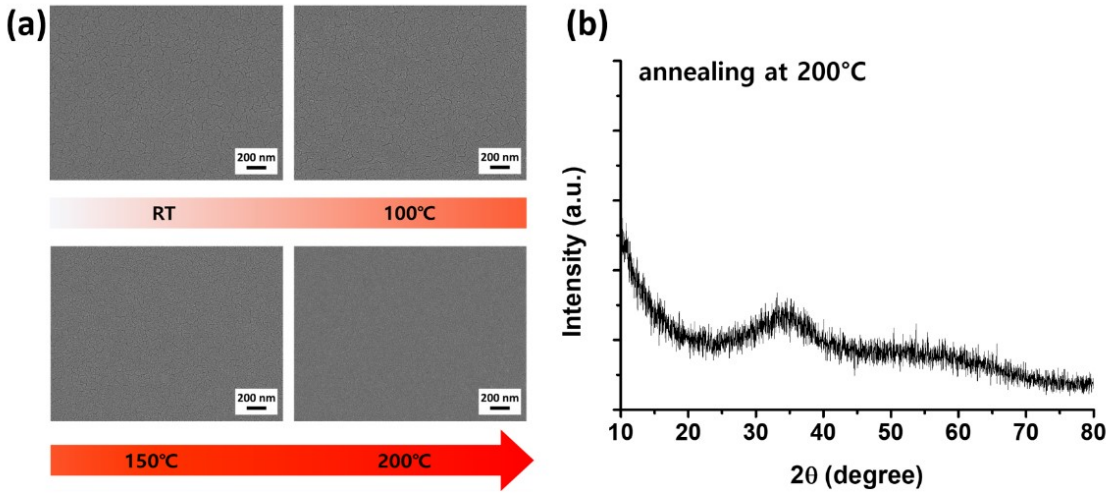

Figure S8. (a) Surface FE-SEM images of RuO_2–OA NP-coated films after annealing at various temperatures for 1 h. (b) Powder X-ray diffraction pattern of the RuO_2–OA NP-coated films after annealing at 200°C for 1 h.

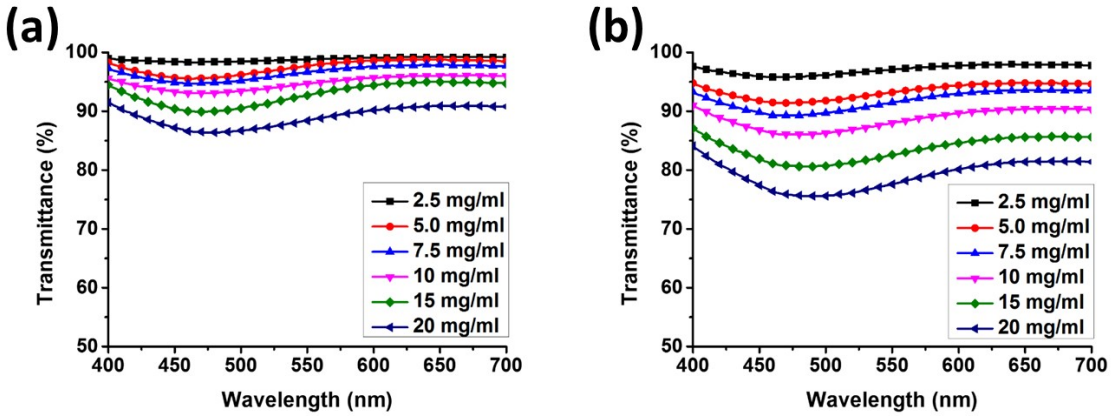

Figure S9. Transmittance spectra of RuO_2 NP-based electrodes prepared by (a) single and (b) double deposition of various NP concentration solutions.

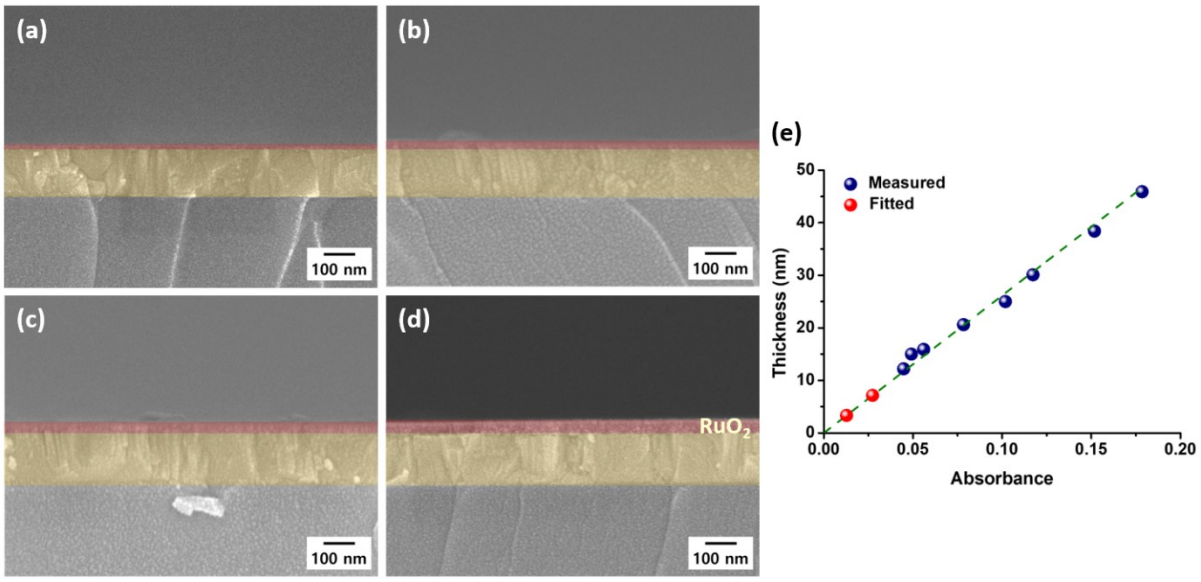

Figure S10. Representative cross-sectional FE-SEM images of RuO_2 NP-based electrodes. The RuO_2 film thicknesses were (a) 15.0, (b) 22.3, (c) 38.4 and (d) 44.5 nm. (e) Plot of measured thicknesses as a function of optical absorbance. The thicknesses of the thinnest two films were determined using their absorbance and the fitting line from the measured data.

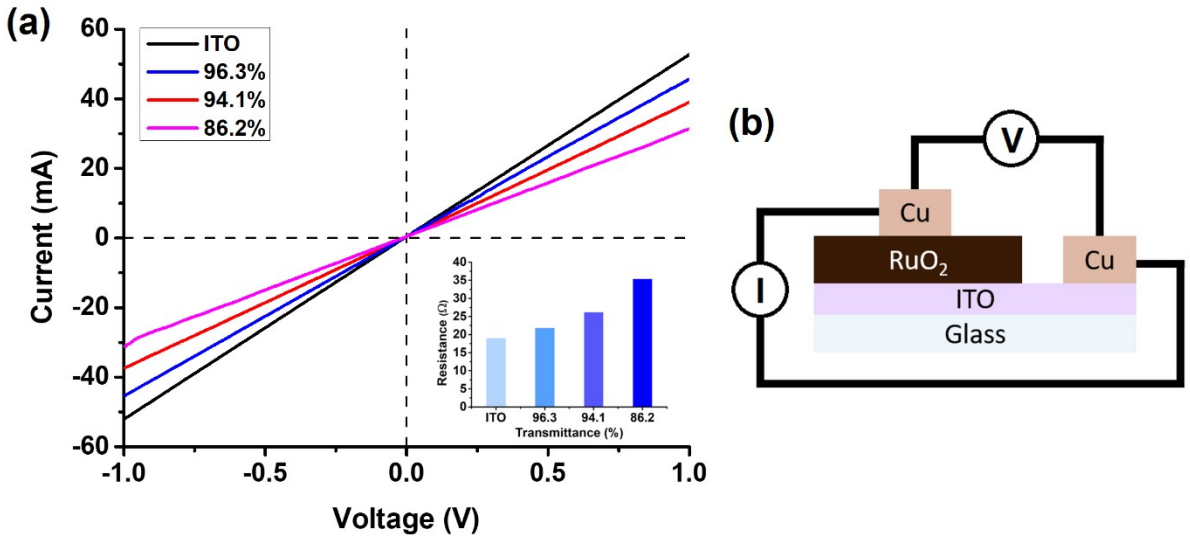

Figure S11. (a) *I-V* characteristics of RuO_2 NP-based electrodes with various optical transmittances (T_{vis}). (b) A schematic illustration of the *I-V* measurement system.

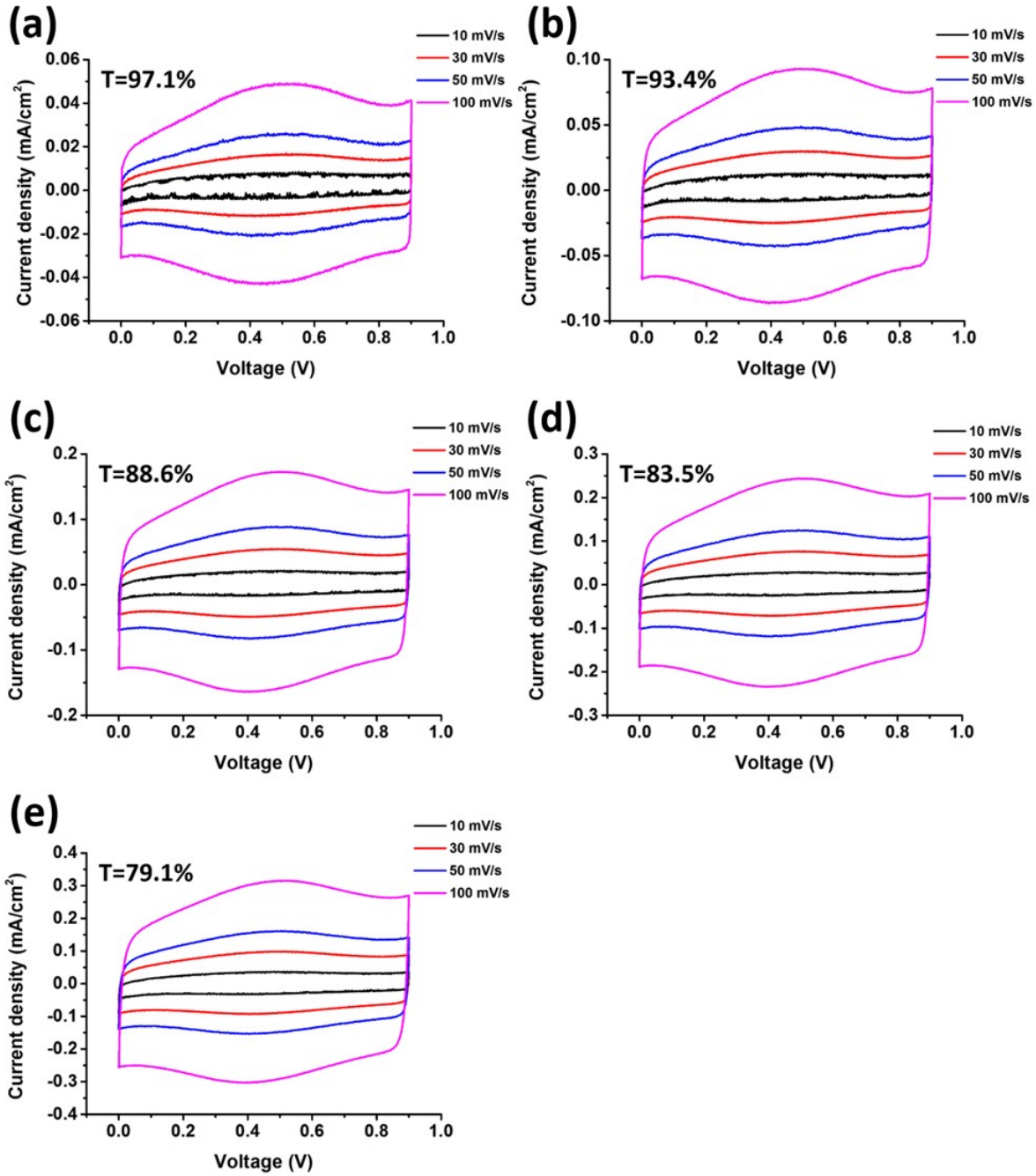

Figure S12. Cyclic voltammograms of RuO_2 NP-based transparent electrodes with T_{vis} of (a) 97.1%, (b) 93.4%, (c) 88.6%, (d) 83.5%, and (e) 79.1% measured at various scan rates.

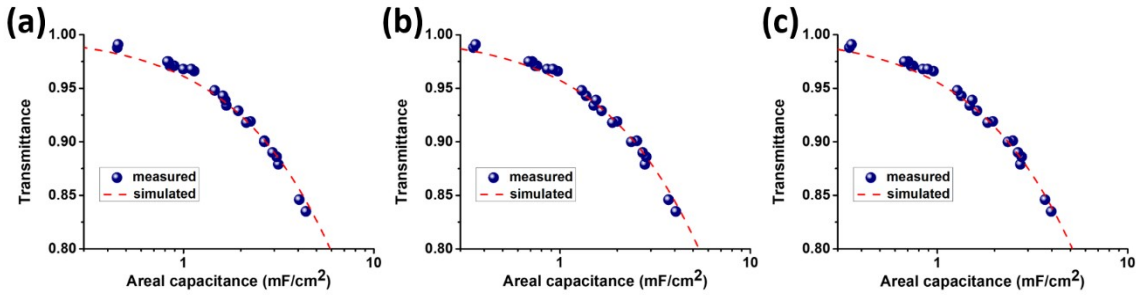

Figure S13. Plots of optical transmittance obtained from experiments (blue points) and simulations using Eq. 2 (red dashed lines) as a function of the areal capacitance at scan rates of (a) 10, (b) 50, and (c) 100 mV/s.

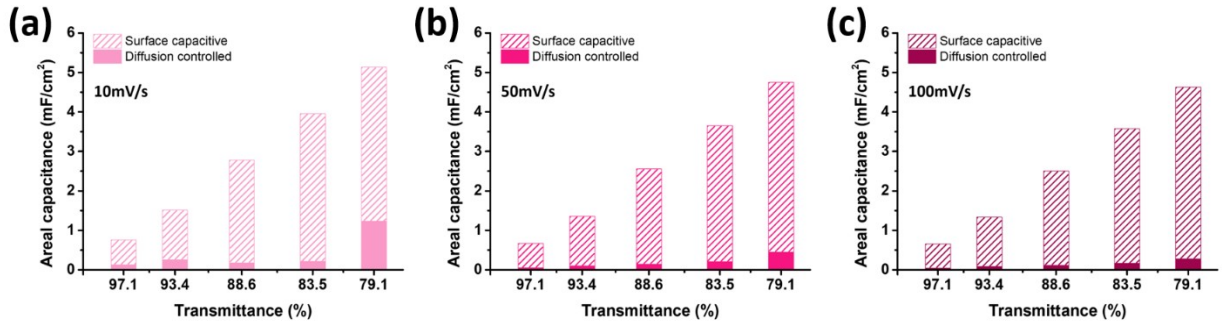

Figure S14. Deconvolution of areal capacitances measured at scan rates of (a) 10, (b) 50, and (c) 100 mV/s for RuO_2 NP-based electrodes with various transmittances. The shaded and solid regions represent surface capacitive and diffusion-controlled insertion elements, respectively.

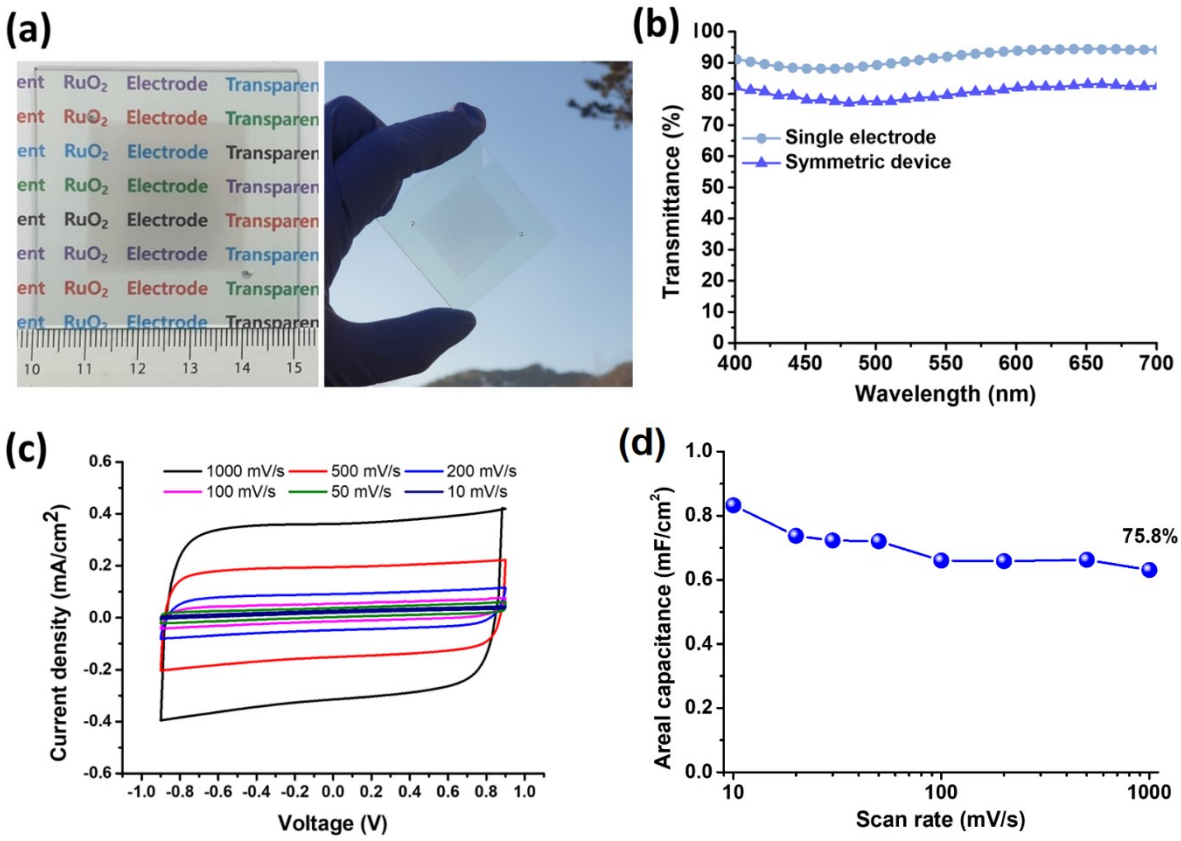

Figure S15. (a) Photographs of the large-area full-cell device fabricated by spray-coating of RuO_2 NPs. (b) Transmittance spectra of a single electrode and symmetric device. (c) Cyclic voltammograms of the device measured at various scan rates. (d) Capacitance retention as a function of the scan rate.

Table S1. Summary of the relative C–H stretching band intensity in FT-IR and the water contact angle of RuO_2–OA NP-coated films after annealing at various temperatures for 1 h.

Annealing temperature (°C)	Relative C-H stretching intensity in FT-IR (%)	Water contact angle (°)
RT	100	89.7
100	91.5	81.9
150	56.5	55.7
200	3.4	36.9

Table S2. Comparison of the optical transmittance and areal capacitance of transparent supercapacitor electrodes and devices in published literature.

Active material	Transmittance (%)	Areal capacitance (mF/cm^2)	Reference
Graphene QD*	93.0	0.009	Nano Energy 26 (2016) 746
Graphene*	75.0	0.101	Chem. Mater. 27 (2017) 3621
SWCNT	92.0	0.552	Nanotech. 27 (2016) 235403
Carbon nanocup*	71.0	1.22	Sci. Rep. 2 (2012) 773
PEDOT:PSS*	65.0	1.18	J. Mater. Chem. A 4 (2016) 10493
Au/MnO_2 network	76.0	3.23	Small 13 (2017) 1701906
RuO_2/N-doped graphene*	34.1	1.57	Sustain. Energy Fuels 2 (2018) 1799
RuO_2/PEDOT	93.0	1.20	Nano Energy 28 (2016) 495
RuO_2 NP	**97.9** **93.4**	**0.85** **1.66**	**This work**

*Data for devices. The others are data for electrodes